Journal of Fundamentals of Renewable Energy and Applications

Okosun and Zhou, J Fundam Renewable Energy Appl 2015, 5:4
DOI: 10.4172/2090-4541.1000174

Research Article Open Access

Computational Examination of Utility Scale Wind Turbine Wake Interactions

Tyamo Okosun and Chenn Q Zhou*

Department of Mechanical Engineering, Purdue University, Center for Innovation through Visualization and Simulation, Purdue University Calumet, USA

Abstract

Numerical simulations of small, utility scale wind turbine groupings were performed to determine how wakes generated by upstream turbines affect the performance of the small turbine group as a whole. Specifically, various wind turbine arrangements were simulated to better understand how turbine location influences small group wake interactions. The minimization of power losses due to wake interactions certainly plays a significant role in the optimization of wind farms. Since wind turbines extract kinetic energy from the wind, the air passing through a wind turbine decreases in velocity, and turbines downstream of the initial turbine experience flows of lower energy, resulting in reduced power output. This study proposes two arrangements of turbines that could generate more power by exploiting the momentum of the wind to increase velocity at downstream turbines, while maintaining low wake interactions at the same time. Simulations using Computational Fluid Dynamics are used to obtain results much more quickly than methods requiring wind tunnel models or a large scale experimental test.

Keywords: Turbine; Kinetic energy; Upstream and downstream

Introduction

Wind energy is a growing source of alternative power in many countries around the world. With many advantages, including a cost per kilowatt hour equivalent to that of an average coal power plant (2.5-3.5 ¢/kWh), wind energy has established itself as an affordable and stable competitor in the energy production market [1]. The earliest recorded machines that harnessed the powter of the wind are the grain grinding mills in Persia [2]. When European travelers and crusaders discovered this technology and brought it to Europe, the transfer of concepts eventually led to the trademark "Dutch" windmill designs, often used to draw water from the ground or grind grain. With the advent of electricity, the next logical evolution in wind power was the wind turbine, which directly converts the kinetic energy of the wind to electricity. A major figure in advancing windmills to create wind turbines in 1891 was the Danish scientist Poul La Cour [3]. In the twentieth century, several countries produced variations of the horizontal axis wind turbine (HAWT) in attempts to create more efficient designs. Compared to drag based designs, these lift based turbines are far more efficient. Even as small scale wind power was experiencing a decline during the 1930s, continued advancements were made in larger scale wind energy generation. In 1941, the collaboration between American engineer Palmer C. Putnam and the Morgan Smith Company of York, Pennsylvania produced the largest wind turbine in the world. This turbine, capable of producing 1.25 MW, would hold that record for almost 40 years. Putnam's goal when designing this turbine was to create a turbine that would be able to produce energy at a rate competitive with common power production methods [4]. It is with this same goal that many utility scale wind turbines are designed today. By 2008 the United States had an estimated capacity of 25000 MW of wind energy. By 2030, the U.S. hopes to use wind power for 20% of its electrical generation requirements [5]. Because of this, there is a considerable need for research dedicated towards the improvement of wind turbine and farm efficiency.

Available wind energy is a significant issue in wind farm arrangement. Because a 1.0 m/s decrease (from 10 m/s to 9 m/s) in wind velocity can result in a 25% drop in power output for a given turbine, it is crucial to site wind turbines such that turbines upstream will not adversely affect the overall performance of the farm. The reduction of available wind power within a farm is usually referred to as a wake or array effect. Since kinetic energy is extracted by each turbine, the air flow exiting a turbine contains less energy for a downstream turbine to extract. By accounting for this effect, a wind farm operator can more accurately decide where to place turbines within a farm to improve energy output. Maintenance costs can also be reduced by accounting for the wake effect, since wakes generated by turbines often induce wind flow outside of ideal design parameters [4].

Wind turbine manufacturers continue to reduce the cost of wind turbines and improve their operating efficiencies, and over the past several decades, the reliability and efficiency of wind turbines have improved greatly. Better wind turbines, in conjunction with a reduction of the overhead costs associated with installing a wind farm and government tax incentives for operations have made wind power more enticing than ever [5]. However, in order to provide electricity at a price that remains competitive with other power production methods, ongoing research within the field of wind energy must be pursued.

Of great importance is the aerodynamic performance of HAWTs. Hansen and Butterfield [6] discussed the research on the aerodynamics of wind turbines and some popular methods of analyzing aerodynamic performance. At the time, the most popular technique for the macro scale analysis of rotors involved Blade Element Momentum (BEM) theory. Due to its ease of use, as well as its accuracy, the BEM method was one of the most widely used methods for examining the flow physics of wind turbine rotors during the end of the twentieth century, and it continued to be the basis for almost all rotor design codes during the past decade [6-9]. While the BEM method provides a ballpark estimation of a rotor's performance, wind tunnel testing is still more accurate at predicting overall power output due to the BEM

***Corresponding author:** Zhou CQ, Professor, Department of Mechanical Engineering, Purdue University, Center for Innovation through Visualization and Simulation, Purdue University Calumet, USA, Tel: 219-989-2665; E-mail: czhou@purduecal.edu

Received April 24, 2015; **Accepted** June 07, 2015; **Published** July 14, 2015

Citation: Okosun T, Zhou CQ (2015) Computational Examination of Utility Scale Wind Turbine Wake Interactions. J Fundam Renewable Energy Appl 5: 174. doi:10.4172/20904541.1000174

method's assumptions regarding complex flow phenomena. Though modifications of the BEM method have been attempted, the inherent assumptions that form the basis of this method's calculations limit its overall accuracy [10].

Combinations of BEM based techniques with the more complex full Navier-Stokes equations are typically more successful than pure modifications of the technique in terms of accuracy. In 2002, Sørensen and Shen [11] developed an aerodynamic model for examining the three dimensional flow field surrounding a wind turbine. The model they developed employs a combination of the three dimensional Navier-Stokes equations and the actuator line technique. Using this technique, they validated the model by performing an analysis of a three bladed 500 kW HAWT. While the BEM methods remain popular for calculating rotor loads and performance, in order to create an accurate depiction of unsteady flow physics, dynamic loading, and other complicated flow physics, more sophisticated methods for examining forces on rotors are needed.

Vortex wake methods have been applied with varying degrees of success to the analysis of wind turbines. Oftentimes, vortex wake methods are implemented into existing analysis models. AeroDyn is currently one of the most popular models for wind turbine design and analysis in the United States. It functions by using a combination of the BEM theories and a simplified variation of the vortex wake methods. However, while fairly accurate, it still lacks the ability to provide complete aerodynamic results, leading to attempts to combine the accuracy of vortex wake models with the speed of AeroDyn [12]. Hugh D. Currin, Frank N. Coton, and Byard Wood [13,14] have developed and validated a new wake model for the analysis of HAWTs. The prescribed vortex wake code *HAWTDAWG*, developed at the University of Glasgow, was linked to AeroDyn and the structural dynamics code FAST in an effort to provide greater accuracy under dynamic flow conditions. The results obtained from this study were compared to experimental Phase VI wind tunnel data, as well as to basic BEM and vortex wake methods built into AeroDyn. *HAWTDAWG* produced results comparable to both the experimental data and the BEM methods during steady, axial flow.

The most accurate numerical method for analysis of fluid flow is directly solving the Navier-Stokes equations governing fluid motion. This is the underlying basis of Computational Fluid Dynamics (CFD). While there are projects geared towards improving currently existing models, with the ever-increasing power of computational systems, using CFD to calculate results based on the Reynolds Averaged Navier-Stokes (RANS) equations has proven to be both accurate and efficient. In 2002, Sørensen et al. [15] completed a RANS simulation of the NREL Phase VI Rotor. The calculated results from this simulation were in good agreement with both BEM methods previously used to model the rotor, as well as with experimental measurements made in the NASA Ames wind tunnel. This simulation also proved that accurate aerodynamic results could be obtained from a 3D CFD simulation. While CFD is more computationally costly than any of the aforementioned methods of analysis, due to advances in modern day computing, CFD is becoming a popular method for analysis when large amounts of detail are required [16].

Currently, there are two major methods of applying CFD for wind turbine analysis. To analyze a given problem, either a commercially available solver can be used or new code can be written and applied. In this project, due to its ease of use and availability, the commercially available CFD package ANSYS Fluent® is used. Various research projects have been conducted using commercial CFD codes, many of which have performed additional validation studies supporting the accuracy of commercial software. One of the most common commercial CFD codes, ANSYS Fluent® is used in many projects due to its flexibility and accuracy. Amano et al. [17] used Fluent® to analyze and improve the design of a wind turbine rotor blade, resulting in the addition of a swept edge to the blade in an effort to extract greater amounts of power from the wind. Palm et al. [18] used Fluent® to determine basic relations that can be used to predict the power output of a given tidal farm configuration.

In 2007, Wußow et al. [19] used ANSYS Fluent® to model a full-sized wind turbine and determine the aerodynamic flow physics in the wake downstream of the rotor. By using a direct model with a body fitted grid, this simulation aimed to accurately capture the flow physics generated by the interaction of rotating turbine blades with a given wind flow. In this case, the rotor rotational speed was fixed at a value corresponding to the velocity of the oncoming wind at the wind turbine hub height. Although this assumption reduces the computational time required for the simulation, it prevents aerodynamic forces from being accurately modeled on the wind turbine rotor. However, this does not affect the downstream wake aerodynamics, which is the main focus of the project. Using the Large Eddy Simulation (LES) turbulence model, Wußow et al. generated results that matched experimental data closely, albeit representing only the lower range of available data. Thus, simplified CFD simulations can provide accurate results in the small time frames encountered in many industrial settings [20].

Several other commercial CFD software packages exist, including ANSYS CFX. CFX was applied by McStravick et al. [21] to analyze the Eppler 423 airfoil as a wind turbine blade. The domain was designed to contain only one blade with periodic boundary conditions to simulate the full turbine. While these other CFD packages exist and have been applied to the analysis of many types of simulations, the popularity and dependability of ANSYS Fluent® make it ideal for the current study.

Objectives

The primary objective of this project is to complete numerical simulations of utility scale wind turbines in two major arrangements designed to optimize energy extraction and decrease the effect of wake losses. From these simulations, the flow physics surrounding the rotors of multiple turbines will be examined. Also, interactions between wind turbines within the simulated wind farms will be examined to determine the effect wakes have on the energy production potential of the proposed siting arrangements. Three major wind farm arrangements will be simulated in this project. The first is a common space saving arrangement. By placing wind turbines in small rows, typically groups of three to five turbines, space is conserved. However, by placing turbines this close to one another, large losses may be induced by wakes. Simulations of this geometry will be used as the baseline.

The second arrangement uses groups of triangularly spaced turbines. As wind passes through a turbine, some of the air cascade around the sides of the turbine. The air passing around the turbine is then forced into the freestream air flow, slightly accelerating the fluid passing around the turbine. By locating turbines in triangular groups, with two turbines placed relatively close downstream and to the left and right sides of the upstream turbine, it is hypothesized that the downstream turbines will be able to generate more power.

The third arrangement is essentially a reversed triangular pattern, or a "delta." The delta simulations are designed to determine if an

increase in velocity in a single turbine downstream of two turbines results in a larger overall increase in power than seen in the triangular arrangement. The project will also attempt to determine any adverse issues with the triangular and delta arrangements by examining various angles of wind flow, as well as the spacing of turbines within a given area. In all of the aforementioned turbine arrangements, the turbines are placed on a flat surface for simulation, similar to a level field with very few trees, or an offshore wind turbine farm.

Theory

CFD numerically solves the complex PDEs known as the Navier-Stokes equations, which govern fluid flow, by discretizing them into a simpler system of algebraic equations that can be easily calculated at various points within a fluid domain. A major concern when analyzing any flow field with CFD is the accuracy of the simulation. Not only can computers introduce rounding errors, results generated by CFD can only be as accurate as the physical models developed to represent fluid flow. Nonetheless, CFD has proven to be an extremely accurate tool for predicting fluid flow in an extremely broad spectrum of applications, including the simulation of wind energy aerodynamics [22].

The simulations performed in this study are run as steady state cases using SIMPLE pressure-velocity coupling. The following methods are used for spatial discretization: 1) least squares cell based gradients, 2) Fluent® standard pressure discretization, and 3) the second order upwind method for momentum, turbulent kinetic energy, and specific dissipation rate. A brief comparison of the wakes generated by transient simulations with those observed in the steady state model was conducted early on in the project. The differences observed in wake formulation are mostly limited to increased vortex generation and vorticity in the wake, with minor variations in velocity. In order to optimize the computational efficiency of the simulations, the steady state model was selected over transient models. Initialization of all cases was performed using Fluent's® hybrid initialization scheme, which solves the Laplace equation to produce an initial velocity field compliant with the boundary domains and cell zone conditions.

Several of the available turbulence models were considered for use in this project, including the Standard k-ε model, the k-ω and k-ω SST models, and more complex models such as the Large Eddy Simulation (LES) and Detached Eddy Simulation (DES) models. The k-ω SST (shear stress transport) model combines the near-wall/vortex accuracy of the k-ω model with the freestream accuracy of the k-ε model. This results in a turbulence approximation model capable of accurately representing the flow physics at the boundary layers surrounding the wind turbine blades, as well as the size, shape, and intensity of the wake as it travels downstream of the turbine.

The LES and DES methods were also examined for use in this project. However, since LES and DES simulations are typically run as transient simulations, they require extremely large computation times. Since the results (size, shape, and position of the turbine wakes) from LES and DES methods differ little from the results from the k-ω SST turbulence model during low turbulence flows, it seems clear that the k-ω SST model is best suited for the simulations in this project [23]. The equations for the k-ω and k-ω SST models are as follows:

Equation for k:

$$\frac{\partial k}{\partial t}+U_j\frac{\partial k}{\partial x_j}=P_k-\beta^* k\omega+\frac{\partial}{\partial x_j}\left[\left(\upsilon+\sigma_k\upsilon_T\right)\frac{\partial k}{\partial x_j}\right]$$

Equation for ω:

$$\frac{\partial \omega}{\partial t}+U_j\frac{\partial \omega}{\partial x_j}=\alpha S^2-\beta\omega^2+\frac{\partial}{\partial x_j}\left[\left(\upsilon+\sigma_\omega\upsilon_T\right)\frac{\partial \omega}{\partial x_j}\right]+2\left(1-F_1\right)\sigma_{\omega 2}\frac{1}{\omega}\frac{\partial k}{\partial x_i}\frac{\partial \omega}{\partial x_i}$$

Numerical Methodology

The design of the wind turbine in this study is based on GE's 1.5 MW utility scale turbines, shown in Figure 1. Since its properties and dimensions are publicly available, this project is able to simulate utility scale wind turbines under realistic operating conditions without the need for proprietary information.

The size, scale, and general operating conditions of this turbine class are available on GE Energy's website.

The blades are based on the popular NREL S809 airfoil with decreasing chord length. The detailed blade design is shown in Figure 2. The blade is also twisted along its length by 22 degrees. A preprocessing software (Gambit®) was used to generate the simulation mesh.

Using this blade design, a three-bladed HAWT is created by attaching the blades to a basic hub and nacelle geometry with a 77 m tower. For each domain, a mesh of roughly 13.5 million cells is generated. The simulations are performed using a rectangular box domain 1.5 km in length, 1 km in height, and 1.5 km in width, with a velocity inlet, pressure outlet, and fixed ground. To simulate the rotor assembly under operating conditions, a cylindrical sliding mesh zone 80 meters in diameter is created surrounding the turbine rotor. This zone is meshed independently of the external flow domain and consists of roughly 1.5 million cells. The cell size near the turbine rotor is specified to be 0.1 meters, expanding at a growth rate of two to 0.5 meters at the outer interfaces. The remaining domain mesh quality is controlled by blocking the domain. The turbine is surrounded by a cube 150 meters per side and the cell size at the turbine tower and nacelle is also specified to be 0.5 meters. The mesh is allowed to expand to a maximum cell

Figure 1: GE's 1.5 MW turbines [24].

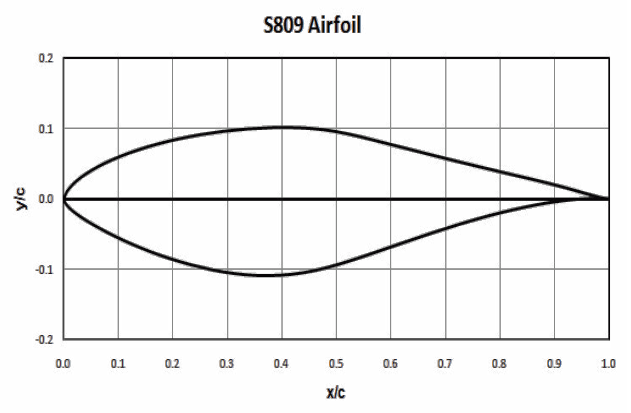

Figure 2: S809 Airfoil [25].

size of 3.5 meters within this zone. Any turbines are then surrounded by a flow block 500 meters wide by 200 meters tall, with a maximum cell size of 7 meters traversing the length of the domain from inlet to outlet. Finally, the remaining domain is meshed as a farfield zone with a maximum cell size of 17 meters. Figure 3 showcases the 3D model of the turbine and the flow domain for simulation.

The next step in creating the geometry is to define the boundary conditions. Boundary conditions define various fluid properties at certain locations within the domain. In this case, since a uniform freestream velocity over the wind turbines of 12 m/s is desired, the velocity inlet boundary condition is set at the inlet face of the domain's large boundary box. This inlet can be set to any given velocity, and it can be varied from case to case. The base simulation inlet speed is 12 m/s, with a turbulent intensity of 5%, and a turbulence length of one meter. The domain outlet is set at the back face of the boundary domain and is defined as a pressure outlet with the pressure at one atmosphere.

The walls and ground of the boundary domain are simple no-slip walls. However, in order to remove the boundary layer on the side and top walls during steady state simulations, they are set to have a constant translational velocity equal to that of the freestream. Therefore, in the base case, the side and top walls move at 12 m/s. This eliminates the wall boundary layer and allows for unimpeded freestream flow.

The wind turbine blades, tower, and nacelle are all basic wall boundary conditions with the no-slip condition, and the volumes are set to specific fluid cell zones. Every volume except the cylindrical volumes surrounding the wind turbine rotor assemblies are defined as stationary fluid zones. The cylindrical volumes are each defined as its own individual fluid zone, so that a sliding mesh rotational speed may be applied in Fluent®.

With the wind turbine geometry determined, the turbines are then placed in various positions for analysis. Three different arrangements of three turbines are simulated in this study. The first arrangement is designed to determine the effects of wakes along a row of wind turbines. The turbines are located 400 m apart and are aligned along the direction of wind flow. The distance between these turbines corresponds to approximately 5 rotor diameters, which is typical on a wind farm. This arrangement can be seen in Figure 4 below.

Two other arrangements are simulated in this study: 1) a triangular arrangement and 2) a reversed triangular arrangement referred to as the delta arrangement. Both of these arrangements are designed with various distances between the turbines in an attempt to determine the impact the upstream turbine wakes have on the intake velocities of the downstream turbines. The base case arrangement for both the triangular and delta setups involves one turbine either 400 m upstream or downstream of two turbines, with the two turbines placed 150 m to either side of the single turbine. In the other cases, the downstream distance between turbines is either increased to 500 m or 600 m and the side to side distance of the two turbines is changed from 100 m to 200 m. Figures 5 and 6 shows an isometric view of both the triangular and delta turbine arrangements.

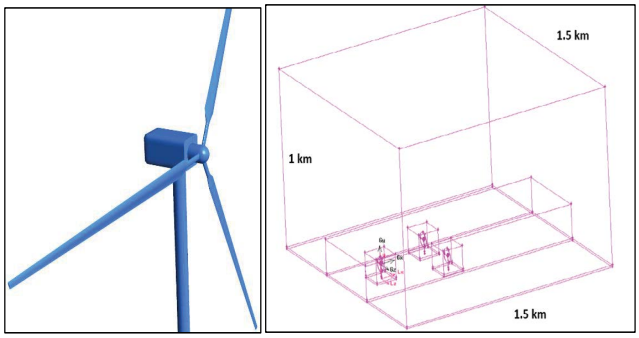

Figure 3: Final wind turbine geometry (left) and an example of a turbine arrangement with domain blocking for mesh design (right).

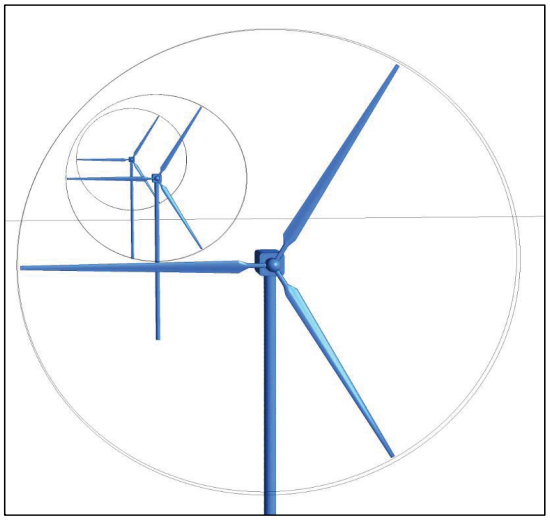

Figure 4: Wind turbines arranged in a row (front view).

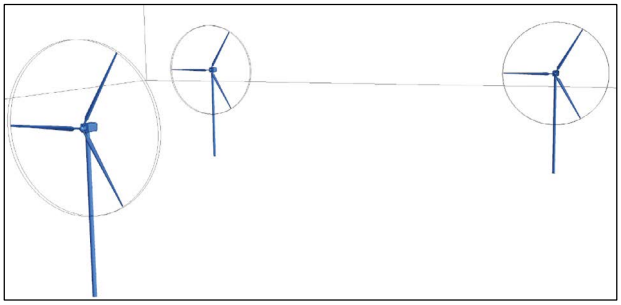

Figure 5: Triangular 400-150 arrangement (isometric view).

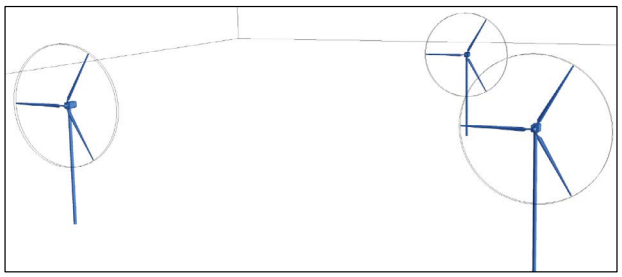

Figure 6: Triangular 400-150 arrangement (front view).

In addition to the direct wind flow geometries, four geometries are created to simulate variations in the incoming angle of the wind. This is done by taking the base case of 400 m by 150 m and rotating the turbines to face an incoming wind flow, which has been turned by a given amount. Then all three turbines are rotated by the same amount about the origin such that they face the inlet of the new geometry. Using this modification, simulations can be conducted using the same flow domain, with turbines interacting as if the incoming wind angle had changed. In this study, both the delta and triangular cases have geometries created for a five and ten degree angle of attack.

A grid sensitivity study, using the 400 by 150 m triangular arrangement, found that decreasing the mesh size below 10 million cells prevented solution convergence. The study also determined that increasing the mesh size above 14 million cells yielded data that did not differ much from the data obtained from k-ω SST simulations, while drastically increasing the computational requirements for timely solution convergence.

Validation

To ensure accurate prediction of airflow surrounding the rotating wind turbine blades, simulations of the 0.66 m chord length S809 wind turbine airfoil experiencing wind flow similar to that at the tip of a wind turbine blade were performed. To achieve validation of the numerical results, a comparison was made with experimental results obtained using a Reynolds number of 2,000,000 corresponding to an inlet velocity of 52.28 m/s. Simulations were conducted at several angles of attack relative to the wind direction. The data is compared to experimental results obtained from the Delft University 1.8 m x 1.25 m low turbulence wind tunnel used by Wolfe and Ochs to validate various CFD models of the S809 airfoil [24-26]. This brief comparison ensures that the basic aerodynamic flow phenomena are accurately represented in the CFD simulation. Figure 7 details the comparison between experimental pressure data measured along the airfoil surface and calculated pressure data from the CFD simulation.

In addition, measurements taken by Barthelmie et al. [27] were used to validate the simulated velocity deficits generated by the wind turbine wakes. Barthelmie et al. used a ship-mounted SODAR to measure wind turbine wakes in an offshore farm in Denmark. The speed profile of the operating turbines was measured and compared with meteorological measurements from nearby masts. The farm contained Bonus Mk III 450 kW wind turbines with rotor diameters of 37 meters. In order to validate the CFD model, a single turbine geometry of matched scale was created.

As observed in Tables 1 and 2, the wake velocities calculated by the CFD model in all cases is either within the error range of the sodar measurements or very close to the range. Also noted by Barthelmie et al. is the fact that wakes meandering cause's errors in the measured data because only a partial wake is measured as opposed to a full wake. Therefore, the CFD models should over-predict wake losses slightly.

Results

In total, 14 different turbine arrangements were simulated, with three different velocities for each geometry (except in the altered wind direction cases) to provide data over a broad spectrum of operating conditions. The turbine row cases were designed to simulate what should be avoided when designing a wind farm with a particular average wind direction in mind. The first inlet velocity is set at the turbine rated speed of 12 m/s with a rotational speed of 15 RPM decreasing down the row. Figure 8 shows velocity contours along a cutting plane viewed from the side, indicating the size and intensity of the wake as it travels downstream. It is obvious from the contours that the wakes experienced by downstream turbines increase in size and intensity as air travels further downstream and encounters more turbines. This view of the contours provides an easy method of visualizing wake size and intensity. However, it does not provide specific information on the losses experienced by the downstream turbines due to the wakes.

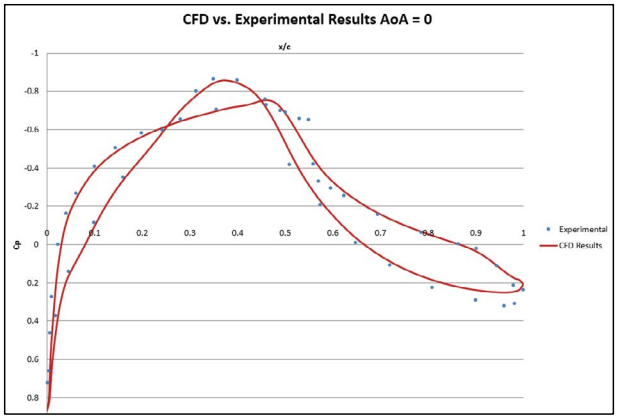

Figure 7: Numerical results vs. experimental results for 0° angle of attack.

Rated Power Output	1.5 MW
Type	Three Bladed, HAWT
Rotor Area	4657 m²
Rotor Diameter	77 m
Tower Height	70 m
Rated Wind Speed, *V*	12 m/s
Rated RPM, *ω*	15 RPM
Maximum Wind Speed	25 m/s
Cut-in Wind Speed	3 m/s

Table 1: Operating and design parameters for GE's 1.5 MW Turbine.

Case	Measured Free-Stream Velocity (m/s)	Rotor Diameters Downstream	SODAR Relative Velocity Deficit (m/s)	CFD Relative Velocity Deficit (m/s)
1	5.74 ± 0.20	2.8	2.28	2.45
2	6.37 ± 0.25	3.4	1.48	2.0
3	6.90 ± 0.59	1.7	4.26	3.1
4	7.54 ± 0.45	2.9	2.57	2.04
5	6.12 ± 0.74	7.4	0.61	1.5
6	8.19 ± 0.46	3.4	2.28	2.34

Table 2: Comparison of measured and calculated wake deficits at turbine hub height.

Figure 9 provides a more quantitative view of the wind velocity as the air travels downstream. The wind speed along the turbine group's centerline shows the velocity deficits after each turbine in detail. The first turbine experiences a wind speed of 12 m/s at the inlet, while the second and third turbines experience wind speeds of approximately 10.5 m/s and 9.7 m/s, respectively. The equation for available wind power is as follows,

Available wind power = $0.5 \times A \times v^3 \times \rho$

Due to the cubic relationship between available wind power and the wind velocity, a 1 m/s decrease in velocity from 10 m/s to 9 m/s can result in an available power decrease of 25%. When examining this simulation, it becomes increasingly clear why minimizing wake losses in wind farms is essential to maintaining the efficiency of the farm. Two additional simulations of this geometry were performed at wind speeds of 10 m/s and 8 m/s. The behavior at these lower speeds is almost identical to the behavior at 12 m/s. The observed velocities from all three cases indicate that the two downstream turbines produce anywhere from 25 to 40% less power compared to the first turbine.

The first triangular geometry simulated was the 400 - 150 m case. This geometry is used as a base case for both the triangular and delta geometries simulated in this project. The cases were simulated at the same three velocities as the three turbine row case: 12 m/s, 10 m/s, and 8 m/s. In this case, there is almost no wake interaction between turbines. Each turbine should experience, at minimum, the inlet velocity of the first turbine. Simulations were performed for both these arrangements to determine if such arrangements might actually increase velocity at the inlets of the downstream turbines, either due to a cascading effect or the funneling of air flow.

Figure 10 shows the velocities at each turbine centerline. There is a small but distinct increase in velocity at both downstream turbines. Before the two turbines (green and blue lines), a 0.042 m/s increase in velocity is observed. While this increase in velocity may appear to be

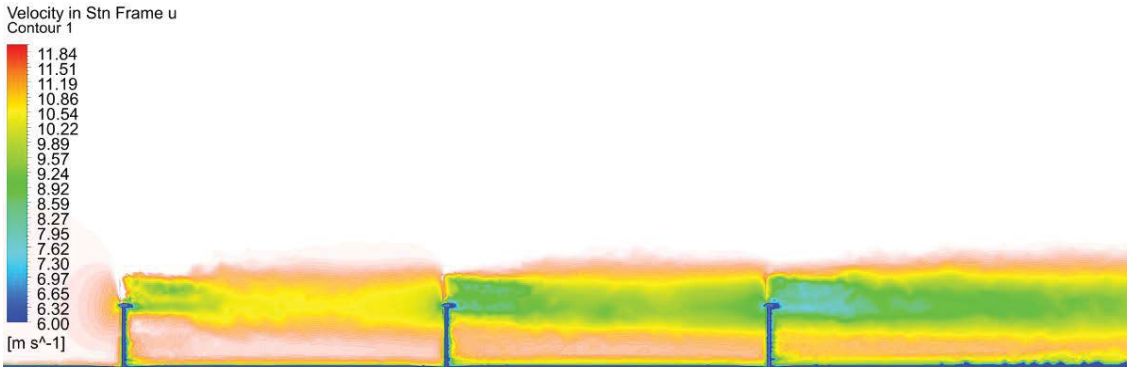

Figure 8: Contours of velocity for the three turbines arranged in a row (12 m/s case).

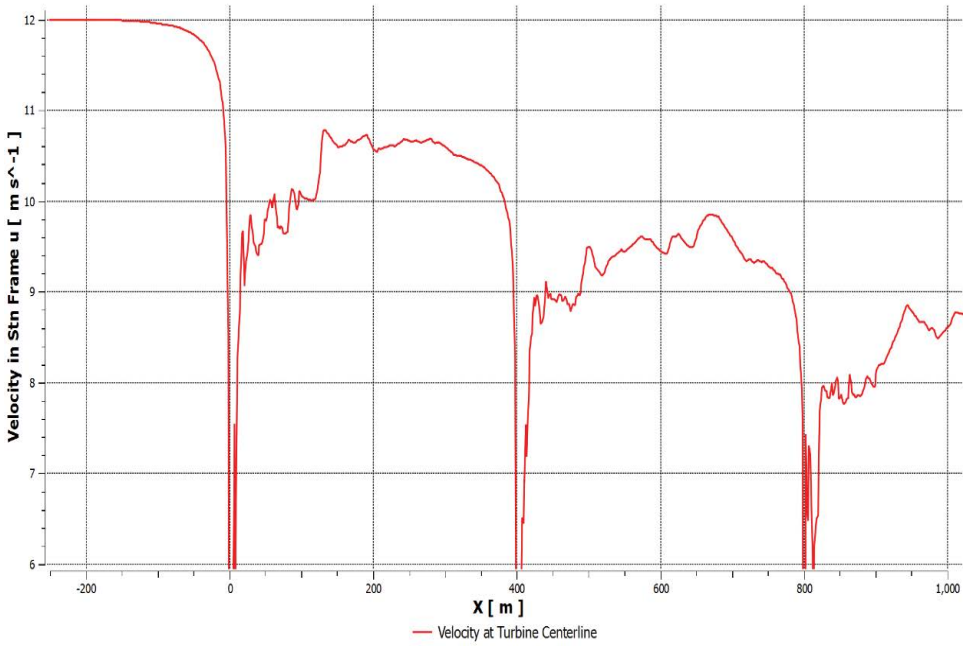

Figure 9: Velocity along the turbine row centerline for the 12 m/s case.

small, the cubic relationship between available wind power and wind speed shows that a 0.042 m/s increase in velocity at 12 m/s results in a 1.05% improvement in performance at each downstream turbine, or a 0.7% increase in energy production for the turbine group when compared to the three individual turbines operating at the given speed. For a group of three 1.5 MW turbines, a 0.7% performance increase results in an additional 32,000 W of power. The 10 m/s and 8 m/s cases result in similar, but smaller, velocity increases.

Figure 11, similar to Figure 10, shows the velocities at turbine centerlines, with the velocity increase at the center turbine visible. The delta cases were simulated to determine if the funneling of air between two wakes could increase energy production. In this case, the velocity increase occurs sooner than in the triangular case, and it is higher, at about 0.061 m/s. While this velocity increase is higher than the increase in speed due to the triangular arrangement, the percent increase in performance for the whole group is lower, at about 0.5%.

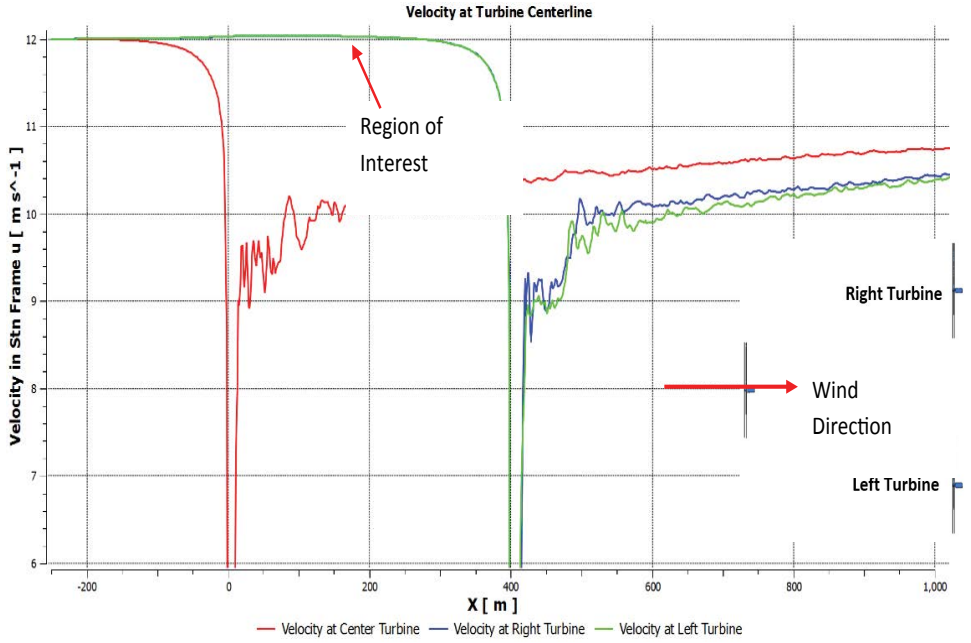

Figure 10: Turbine centerline velocities for the 400-150 m triangular case at 12 m/s.

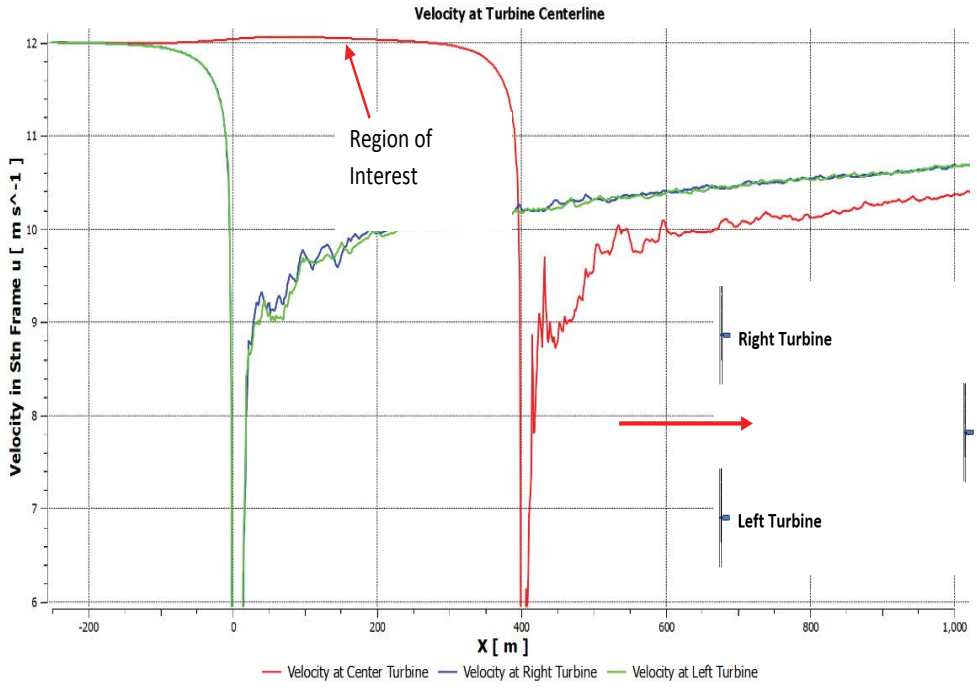

Figure 11: Turbine centerline velocities for the 400-150 m delta case at 12 m/s.

Similar results were observed for the delta cases when the wind speed was reduced.

When the wind direction is changed, wake interactions become much more significant. In fact, changes in wind direction completely negate any performance gains from the arrangement of the turbines. Therefore, in order to take maximum advantage of the arrangements presented in this study, the wind farm site should be located in a region with very little variability in wind direction. Figure 12 below shows an example of the velocity contours generated by one of the four simulated wind direction cases.

As seen in Figure 12, the left downstream turbine experiences a waked flow at half of its rotor inlet speed, which leads to both reduced power output from the turbine and additional fatigue stress due to the varying velocities at the turbine inlet.

From the simulations, it was determined that, in general, the triangular cases are more efficient than the delta arrangements at corresponding velocities. Also, the triangular 400 m by 100 m geometry produced the largest overall performance gains for the turbine group, with the triangular case remaining slightly more effective at increasing total power output than the delta case. The performance levels of the turbine group geometries are shown in Figure 13 and Table 3 below. The performance increases were determined by using the available wind power equation to calculate the percent increase in available wind power at each turbine experiencing the velocity increase. The power increases were then averaged over the group of three turbines to determine the percent performance increase for the group as a whole, and by extension, for a wind farm using the given arrangement.

As mentioned before, the 400 m by 100 m simulations showed the largest performance gains compared to turbines experiencing the given speeds individually or without influence from a grouping, such as ones in a parallel row. The four simulations conducted with various wind directions indicated that the benefits of the triangular or delta arrangements are most pronounced when the wind travels directly downstream. If the wind direction changes roughly 10 to 15° at a given site, the 400 by 150 m cases can cause certain turbines to become waked, resulting in the negation of any performance improvements due to the geometry.

Conclusion

This study proposes a possible method of generating more power from wind turbines by arranging turbines in either triangular or delta groups, arrangements designed to increase wind flow at rotor inlet planes by either cascading flow around a single leading turbine or by funneling it through the area between two turbine wakes. To investigate the appropriateness of each arrangement, several CFD simulations of

Figure 12: Velocity contours for a 400 – 150 m triangular arrangement with the wind direction at 10°.

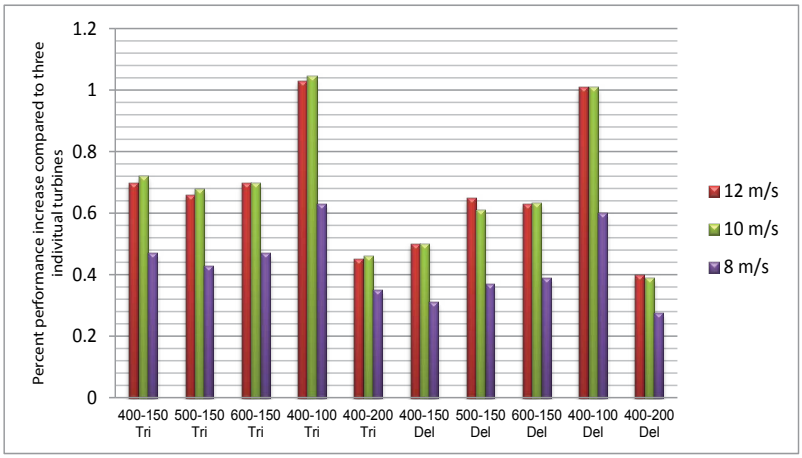

Figure 13: Graph of percent performance increase in each simulation geometry.

Case	12 m/s	10 m/s	8 m/s
400 - 150 m Tri.	0.7%	0.72%	0.47%
500 - 150 m Tri.	0.66%	0.68%	0.43%
600 - 150 m Tri.	0.7%	0.7%	0.47%
400 - 100 m Tri.	1.03%	1.045%	0.63%
400 - 200 m Tri.	0.45%	0.46%	0.35%
400 - 150 m Del.	0.5%	0.5%	0.31%
500 - 150 m Del.	0.65%	0.61%	0.37%
600 - 150 m Del.	0.63%	0.634%	0.389%
400 - 100 m Del.	1.01%	1.01%	0.6%
400 - 200 m Del.	0.4%	0.39%	0.275%

Table 3: Recorded values of performance increase in simulation cases.

various turbine geometries were performed. Each geometric variation was simulated at three different velocities at the domain inlet (12 m/s, 10 m/s, and 8 m/s) to simulate the various wind speeds that might be encountered by turbines operating in a farm. In addition, four extra simulations were performed to determine the effects of wind direction.

The results of this study indicate that the triangular arrangements produce more energy than the delta arrangements. This is primarily due to the increase in velocity at the two rear turbines in the triangular arrangement, as opposed to an increase in velocity at only a single rear turbine in the delta cases. Of all the arrangements, the 400 m by 100 m triangular arrangement yielded the best results, with a performance increase of 1.05%, which could lead to an additional 47,000 W of power. Theoretically, in a utility scale wind farm capable of producing 200 MW of power, this performance increase applied to the entire farm would result in an increase in power generation about of 2.1 MW. If the given 200 MW wind farm has an installation cost of $100,000,000, the cost per MW of energy production capacity at installation is $500,000. Using the triangular groupings, the power production capacity would increase to 202.1 MW, resulting in a cost per MW value of about $494,070. Therefore, through the use of the triangular arrangement, the initial cost per MW of power generation capacity is reduced by approximately 1.1%. In the case described above, this translates to an overall savings of $6000 saved per MW of capacity installed.

However, this performance increase is not without certain drawbacks. Since the turbines are placed relatively close together, the possibility of intense turbulence from wake interactions is significantly higher. Also, in sites where the wind shifts direction frequently, the benefits of the triangular arrangement are significantly diminished. In fact, additional maintenance costs might be incurred if certain wind directions result in the upstream turbine directly waking one of the downstream turbines. Finally, all simulations were performed with the assumption that the turbines sat on completely level ground, such as a large field with few trees or an offshore farm. Therefore, the results may have little bearing on sites when terrain obstructions are present. In summary, these arrangements are recommended for use in utility scale farms only when the average annual wind direction is fairly consistent and the land is relatively level.

Acknowledgements

This research was supported in part by US Department of Energy Grant DE-EE0003265 and US Department of Education Grant P116B100322. However, the contents do not necessarily represent the policy of the U.S. Department of Education, and endorsement by the Federal Government should not be assumed.

References

1. NREL (2005) Wind Energy Myths, Report No. DOE/GO-102005-2137, U.S. Department of Energy.
2. Thomas BG, Urquhart J. (1996) Wind Energy for the 1990's and Beyond. J Energy Convers Manag 37: 1741.
3. Liu R, Ting, David K (2003) On the Aerodynamics of Wind Turbine, Proceedings of the 2003 International Joint Power Generation Conference, ASME, Atlanta, GA, USA.
4. Spera DA (2009) Wind Turbine Technology: Fundamental Concepts of Wind Turbine Engineering, ASME Press, New York, NY: 41 - 43, 83 - 87, 198 - 199.
5. Jha AR (2011) Wind turbine technology. CRC Press, Boca Raton, FL: 9 - 15.
6. Hansen AC, Butterfield CP (1993) Aerodynamics of Horizontal-Axis Wind Turbines. Ann Rev Fluid Mech 25: 115 - 149.
7. Vermeer LJ, Sørensen JN, Crespo A (2003) Wind Turbine Wake Aerodynamics. Prog Aerospace Sci 39: 467 - 510.
8. Kulunk, E, Yilmaz, N (2009) Aerodynamic Design and Performance Analysis of HAWT Blades, Proceedings of the ASME 2009 Fluids Engineering Division Summer Meeting, ASME, Vail, CO, USA.
9. Refan M, Hangan H (2010) Experimental and Theoretical Study of the Aerodynamic Performance of a Small Horizontal Axis Wind Turbine. ASME 2010 Power Conference, ASME, Chicago, IL, USA.
10. Haans W, Sant T, van Kuik G, van Bussel G (2006) Stall in Yawed Flow Conditions: A Correlation of Blade Element Momentum Predictions With Experiments. J Solar Energy Engg 128: 472 - 480.
11. Sørensen JN, Shen WZ (2002) Numerical Modeling of Wind Turbine Wakes. J Fluids Engg 124: 393 - 399.
12. Currin HD, Long J. (2009) Horizontal Axis Wind Turbine Free Wake Model for AeroDyn. Oregon Institute of Technology, Klamath Falls, OR, USA.
13. Currin HD, Coton FN, Wood B (2008) Dynamic Prescribed Vortex Wake Model for AERODYN/FAST. J Solar Energy Engg 130.
14. Currin HD, Coton FN (2007) Validation of a Dynamic Prescribed Vortex Wake Model for Horizontal Axis Wind Turbines. Proceedings of the 5th Joint ASME/JSME Fluids Engineering Conference, ASME, San Diego, CA, USA.
15. Sørensen JN, Michelsen JA, Schreck S (2002) Navier-Stokes Predictions of the NREL Phase VI Rotor in the NASA Ames 80 ft x 120 ft Wind Tunnel. Wind Energy 5: 151 - 169.
16. Anderson JD (1995) Computational Fluid Dynamics: The Basics with Applications. McGraw-Hill, Inc, New York, NY.
17. Amano RS, Malloy RJ (2008) Aerodynamic Comparison of Straight Edge and Swept Edge Wind Turbine Blade. ASME International Mechanical Engineering Congress and Exposition, ASME, Boston, MA, USA.
18. Palm M, Huijsmans R, Pourquie M, Sijtstra A (2010) Simple Wake Models for Tidal Turbines in Farm Arrangement. ASME 2010 29th International Conference on Ocean, Offshore and Arctic Engineering, ASME, Shanghai, China.
19. Wußow S, Stizki L, Hahm T (2007) 3D-Simulation of the Turbulent Wake Behind a Wind Turbine. J Physics 75.
20. De Bellis F, Catalano LA, Dadone A (2010) Fast CFD Simulation of Horizontal Axis Wind Turbines. ASME Turbo Expo 2010: Power for Land, Sea and Air, ASME, Glasgow, UK.
21. McStravick DM, Houchens BC, Garland DC, Davis KE (2010) Investigation of an Eppler 423 Style Wind Turbine Blade. ASME 2010 4th International Conference on Energy Sustainability, ASME, Phoenix, AZ, USA.
22. Wendt JF (2009) Computational Fluid Dynamics: An Introduction. Springer-Verlag Berlin Heidelberg.
23. Versteeg H, Malalasekra W. (2007) An Introductions to Computational Fluid Dynamics: The Finite Volume Method. McGraw-Hill, Inc, New York, USA.
24. www.en.wikipedia.org/wiki/GE_Wind_Energy#GE_1.5MW
25. http://wind.nrel.gov/airfoils/Shapes/S809_Shape.html
26. Wolfe WP, Ochs SS (1997) CFD Calculations of S809 Aerodynamic Characteristics. AIAA paper 97-0973.
27. Barthelmie RJ, Folkerts L, Larsen GC, Rados K, Pryor SC, et al. (2006) Comparison of Wake Model Simulations with Offshore Wind Turbine Wake Profiles Measured by Sodar. J Atmospheric Oceanic Technol 23: 888 – 901.